



Subject Areas:

planetary science, solar system, giant planets

Keywords:

Ice giants, protosolar nebula, volatiles

Author for correspondence:

Olivier Mousis

e-mail: olivier.mousis@lam.fr

The role of ice lines in the formation of Uranus and Neptune

O. Mousis¹, A. Aguichine¹, R. Helled²,
P.G.J. Irwin³, and J.I. Lunine⁴

¹Aix Marseille Univ, CNRS, CNES, LAM, Marseille, France

²Center for Theoretical Astrophysics & Cosmology
University of Zurich, Winterthurerstr. 190, CH-8057 Zurich Switzerland

³Department of Physics (Atmospheric, Oceanic and Planetary Physics), University of Oxford, Parks Rd, Oxford OX1 3PU, UK

⁴Department of Astronomy, Cornell University, Ithaca, NY 14853, USA

We aim at investigating whether the chemical composition of the outer region of the protosolar nebula can be consistent with current estimates of the elemental abundances in the ice giants. To do so, we use a self-consistent evolutionary disk and transport model to investigate the time and radial distributions of H₂O, CO, N₂, and H₂S, i.e., the main O-, C-, N, and S-bearing volatiles in the outer disk. We show that it is impossible to accrete a mixture composed of gas and solids from the disk with a C/H ratio presenting enrichments comparable to the measurements (~70 times protosolar). We also find that the C/N and C/S ratios measured in Uranus and Neptune are compatible with those acquired by building blocks agglomerated from grains and pebbles condensed in the vicinities of N₂ and CO ice lines in the nebula. In contrast, the presence of protosolar C/N and C/S ratios in Uranus and Neptune would imply that their building blocks agglomerated from particles condensed at higher heliocentric distances. Our study demonstrates the importance of measuring the elemental abundances in the ice giant atmospheres, as they can be used to trace the planetary formation location and/or the chemical and physical conditions of the protosolar nebula.

1. Introduction

Uranus and Neptune are the outermost giant planets of our solar system. The apparent size of these two planets in the sky is roughly a factor of 10 smaller than Jupiter and Saturn, making their physical properties much more difficult to characterize. The bulk compositions of Uranus and Neptune are poorly known [1]. Interior models suggest that these planets contain $\sim 10\text{--}25\%$ of H-He by mass, where the exact number depends on the assumed composition of the heavy elements [2]. Therefore, although there are estimates for the total heavy-element mass, the available data are insufficient to discriminate among different elemental compositions, implying that the water-to-rock ratio remains unknown. Often models assume a large region of the planet presenting high volatiles enrichments [3–6]. This is supported by the measurement of the C abundance, found to be enriched ~ 70 times its protosolar value in both planets (see Table 1), but recent measurements suggest that N/H and S/H ratios might be instead subsolar in their envelopes [7,8], unless hidden reservoirs of nitrogen and sulfur exist at deeper levels [9,10]. At present, it remains unclear whether the measured C abundance represents the planetary bulk. Often it is assumed that this is the case, which corresponds to fully mixed (convective) planetary interiors but increasingly models assume that both Uranus and Neptune are not fully mixed, and contain composition gradients and/or boundary layers, making the connection between the atmospheric and bulk composition challenging. Nevertheless, it remains useful to use the measured abundances, and link them to possible formation locations.

To explain the apparent discrepancy observed between the C and N abundances in their envelopes, it has been proposed that Uranus and Neptune have grown from N-depleted building blocks at the location of the carbon monoxide ice line [11]. However, this scenario did not consider the possibility that the measured N abundance could be simply a lower limit in Uranus and Neptune, a hypothesis which has been proposed since then [9,12]. The model also overestimated the redistribution of volatiles around their ice lines for two reasons. First, calculations of volatiles transport were based on a stationary PSN model while the thermodynamic conditions in disks evolve significantly over the first hundred thousand years. Second, instantaneous condensation of vapors was assumed, instead of using condensation rates, thus leading to an overly efficient production of solids in the vicinity of the ice lines.

In this paper, we investigate whether the chemical composition of the outer region of the PSN is consistent with current estimates of the elemental abundances in the ice giants by overcoming the afore-mentioned issues. We use a self-consistent evolutionary disk and transport model to investigate the time and radial distributions of H_2O , CO, N_2 , and H_2S , i.e. the main O-, C-, N-, and S-bearing volatiles in the outer PSN [13]. The calculated abundance profiles in the outer part of the disk are then compared with the abundance data available for the two planets. Section 2 is dedicated to a short description of the existing abundance data of species of interest in the atmospheres of the ice giants. The disk and transport model used is summarized in Section 3. Section 4 presents the calculated abundances profiles in the outer PSN and the comparisons with the compositions of Uranus and Neptune. Our conclusions are presented in section 5.

2. Abundances of heavy elements in Uranus' and Neptune's atmospheres

The composition of the deep atmospheres of Uranus and Neptune is shrouded in mystery since most of heavy constituents condense at pressures deeper than can readily be probed remotely. Water is expected to condense at very deep pressures ($\gg 100$ bar) and ammonia and hydrogen sulphide are expected to combine together to form a cloud of either NH_4SH or $(\text{NH}_4)_2\text{S}$ at a pressure of 40–50 bar, leaving the more abundant gas (i.e., either NH_3 or H_2S) to condense at lower pressures (< 10 bar). Finally, methane is predicted to condense at a pressure of 1–2 bar (depending on abundance). For Jupiter and Saturn, the abundance of NH_3 appears to exceed that of H_2S since gaseous ammonia is detected at the cloud tops. However, the situation in

the atmospheres of Uranus and Neptune has been less clear. Observations of the microwave spectrum of Uranus and Neptune showed it to be much brighter than expected, suggesting that the abundance of NH_3 (which is a strong microwave absorber) was depleted [14–16], leading to the suggestion that the abundance of H_2S exceeded that of NH_3 at 40–50 bar, and that H_2S should be present alone at lower pressures and condense at about 3 bars. This presence of H_2S gas absorption features above the clouds of both Uranus and Neptune has recently been detected in Gemini/NIFS observations [7,8], which support this hypothesis. One explanation for the apparently low abundance of ammonia in the atmospheres of Uranus and Neptune is that it is partially dissolved in an aqueous ammonia cloud. However, this is not predicted to be able to absorb sufficient ammonia and it has been suggested that ammonia (and hydrogen sulphide) may instead partially dissolve in a water “ocean” or even in an “ionic ocean” at depth (e.g., [9]), modifying the apparent deep abundance of nitrogen and sulphur in the atmospheres of Uranus and Neptune. Alternatively, if we believe the observed abundances of H_2S and NH_3 to be representative of the bulk composition of these worlds, then it suggests that Uranus and Neptune may have formed in a colder part of the solar nebula than Jupiter and Saturn, in a region where more S than N was accreted into the planets [7,8].

Finally, a potential clue to the deep abundances of Uranus and Neptune comes from the observations of carbon monoxide, which resides mostly in the stratosphere, but which may perhaps have also been detected in the upper troposphere. On Uranus, CO estimates suggest abundances of 7.1–9.0 ppb in the stratosphere [17], and a $3\text{-}\sigma$ upper limit of 2.1 ppb in the troposphere for pressures 0.1–0.2 bar [18]. The abundance of CO in Neptune’s atmosphere is even found to be much higher with [19] determining a step-type profile with 1–2 ppm in the stratosphere and 0–0.3 ppm in the troposphere at pressures > 1 bar. The presence of CO in the stratosphere can be explained through the impact of comets or via interplanetary dust particles, but models that can predict such high abundances in the troposphere need to have atmospheric compositions that are heavily enriched in O/H by at least 280 times solar [17,19,20]. However, such a large enrichment of O/H is not compatible with D/H measurements, which suggest more modest O/H enrichments of $\sim 50\text{--}150$ [25] if Neptune’s internal water was sourced from protoplanetary ices with D/H comparable to present day comets. These considerations point toward how challenging it is to derive the O/H ratio from CO [9], **as also noted by Teanby et al. [This issue]**. Given those difficulties, the present work only takes into account the measurements of C, N, and S in the envelopes of Uranus and Neptune (see Table 1).

Table 1: C, N, and S abundance ratios in the Sun, Uranus and Neptune

Elements	Sun-Protosolar ^a	Uranus/Protosolar	Neptune/Protosolar
C/H	2.95×10^{-4}	$70 \pm 35^{(b)}$	$70 \pm 35^{(b)}$
N/H	7.41×10^{-5}	$> (\sim 0.08\text{--}0.2)^{(c)}$	$(\sim 0.02\text{--}0.08)^{(c)}$
S/H	1.45×10^{-5}	$> (\sim 0.4\text{--}1.0)^{(c)}$	$> (\sim 0.1\text{--}0.4)^{(c)}$

(a) Protosolar values based on the solar photospheric values of [21]; (b) based on estimated upper tropospheric abundance of CH_4 on Uranus and Neptune’s atmospheres of 0.04 [22–24]; (c) from estimates of upper tropospheric H_2S in the atmospheres of Uranus and Neptune [7,8] and assuming $\text{S/N} > 4.5\text{--}5 \times \text{solar}$.

3. Volatile distribution model

The volatile transport and distribution model used in our work is derived from the approach described in [26], to which the reader is referred for details. In a few words, our time-dependent PSN model is governed by the following differential equation [27]:

$$\frac{\partial \Sigma_g}{\partial t} = \frac{3}{r} \frac{\partial}{\partial r} \left[r^{1/2} \frac{\partial}{\partial r} \left(r^{1/2} \Sigma_g \nu \right) \right]. \quad (3.1)$$

This equation describes the time evolution of a viscous accretion disk of surface density Σ_g of viscosity ν , assuming hydrostatic equilibrium in the z direction. The viscosity is calculated in the framework of the α -formalism [28] using the following method. For each distance r to the Sun, the disk's properties are calculated by solving the equation of energy balance between viscous heating and radiative transfer at the midplane level. This gives us ν , as well as the pressure and temperature profiles of the disk as a function of r . The evolution of the disk is started with an initial profile given by $\Sigma_g \nu \propto \exp(-r^{2-p})$, with $p = \frac{3}{2}$ for an early disk [27]. In our computations, $\alpha = 5 \times 10^{-3}$ and the disk mass is set equal to $0.1 M_\odot$. 99% of the disk mass is encapsulated within ~ 100 AU and the initial mass accretion rate onto the Sun is set to $10^{-7.6}$ [29].

The size of dust particles used in our model is determined by a two-populations algorithm derived from [30]. This algorithm computes the representative size of particles through the estimate of the limiting Stokes number in various dynamical regimes. In our model, dust is initially present in the form of particles of sizes $a_0 = 10^{-7}$ m, and grow through mutual collisions. This growth is limited by the maximum sizes imposed by fragmentation or by the drift velocity of the grains (see [26] for details). The dust surface density is the sum over all surface densities of available solids at given time and location, assuming a protosolar ice-to-rock ratio (~ 2.57) [31], and a bulk density of 0.5 for rocks and 0.15 for ices. The two latter values correspond to the formation of aggregates made from the random deposition of irregular particles made of olivine ($\rho = 3300 \text{ kg m}^{-3}$) and ices ($\rho = 1000 \text{ kg m}^{-3}$), with a 15% filling factor [32].

We follow the approaches of [33, 34] for the dynamics of trace species in term of motion and thermodynamics, respectively. We assume that all trace species are entirely independent in our simulations and that the disk is uniformly filled with H_2O , CO , N_2 and H_2S . These molecules are considered to be the dominant volatile species in the PSN, assuming protosolar abundances for O, C, N, and S [21]. Half S is assumed to be in H_2S form with the other half forming refractory sulfide components [35], and all C forms CO with the remaining O going into H_2O . No chemistry is assumed to happen between the trace species. Sublimation of grains occurs during their inward drift when partial pressures of trace species become lower than the corresponding vapor pressures. Once released, vapors diffuse both inward and outward. Because of the outward diffusion, vapors can recondense back in solid form following the rates defined by [34], and condensation occurs either until thermodynamic equilibrium is reached or until no more gas is available to condense. The motion of dust and vapor is computed by integrating the 1D radial advection-diffusion equation derived from [30,33], and detailed in [26]. The vapor pressures of trace species are taken from [36].

4. Results

Figure 1 represents the radial profiles of oxygen, carbon, nitrogen, and sulfur enrichments relative to their protosolar values [21], both in vapor and solid phases, and at different epochs of the PSN evolution. The vapor and solid oxygen enrichment profiles correspond to the sum of H_2O and CO contributions. At $t = 0$, each O enrichment profile in gaseous and solid forms follow two plateaus. These plateaus are delimited by drops of enrichments corresponding to the presence, with progressing heliocentric distance, of the H_2O and CO icelines. With time, the ice lines move inward the disk. At 0.1 Myr, two peaks of solid oxygen form immediately after the icelines. These peaks correspond to the formation of ices resulting from the backward diffusion of vapors. Two

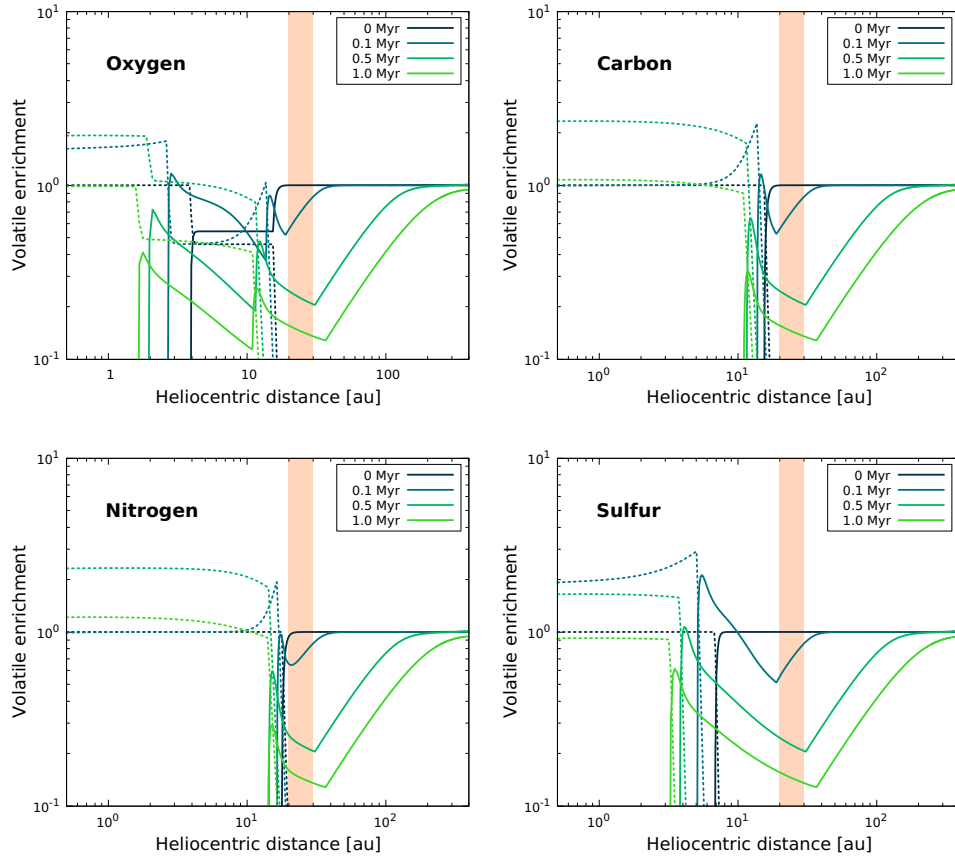


Figure 1: Radial profiles of oxygen, carbon, nitrogen, and sulfur enrichments relative to their protosolar values, as a function of time in the PSN. Dashed and solid lines correspond to vapor and solid phases, respectively. The orange area encompasses the current locations of the ice giants in the solar system.

peaks of vapors also appear along the ice lines, as a result of the sublimation of drifting ices. With time, the O abundance in vapor form increases in the inner disk until it reaches a plateau corresponding to \sim twice the protosolar value at 1 Myr. In contrast, the O abundance in solid form decreases with time and heliocentric distance beyond the peaks formed after the H₂O and CO ice lines in the outer disk. In this case, the O abundance drastically varies with heliocentric distance but always remains subsolar.

The behavior of the enrichment profiles of C-, N-, and S-bearing species is simpler in our calculations because they individually only depend on one species. Peaks of vapors and solids quickly form to the left and right of the ice lines, respectively. The three panels share the same features with a moderate enrichment (about 2–3 times protosolar at most) of the vapors present in the inner disk and a significant depletion of the solids in the outer disk. The figure shows it is not possible to accrete a mixture composed of gas and solids with a C/H ratio presenting enrichments comparable to the values (\sim 70 times protosolar) measured in the atmospheres of Uranus and Neptune. This suggests that the formation of Uranus and Neptune from disk instability [37] is rather unlikely, unless a postformation mechanism, such as photoevaporation, has increased the metallicities of the planets [38]. Instead, one should expect formation of these giants by the concurrent accretion of gas and solids by migrating embryos [39,40], provided the accreted mixtures shared a composition consistent with those of Uranus and Neptune.

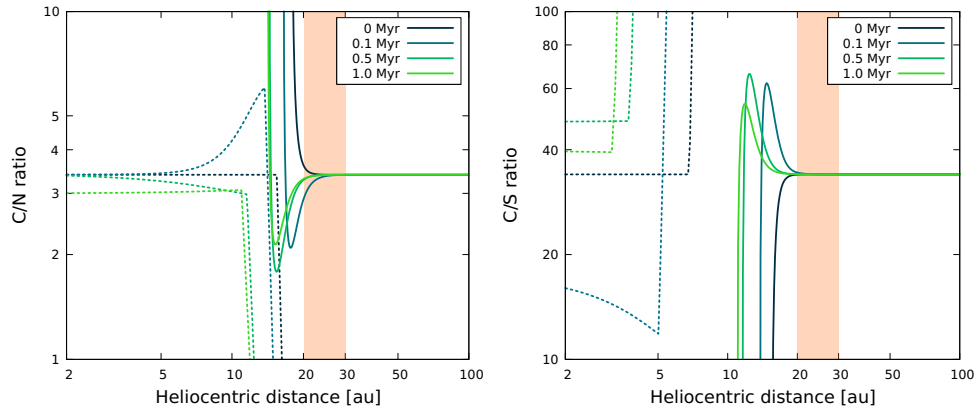


Figure 2: Radial profiles of the C/N and C/S ratios at different epochs of the PSN evolution. Dashed and solid lines correspond to vapor and solid phases, respectively. The orange area encompasses the current locations of the ice giants in the solar system.

Figure 2 shows the time evolution of the C/N and C/S ratios radial profiles throughout the PSN. Very high C/N and C/S ratios can be obtained in solid forms in the 10–20 AU region of the PSN, i.e. the location where the ice lines are at play. In contrast, these ratios, still in solid phase, remain protosolar ($(C/N)_{\odot} \simeq 3.4$ and $(C/S)_{\odot} \simeq 17.8$) at higher heliocentric distances, irrespective of the epoch considered. While the inner regions of the PSN cannot be considered as a viable formation region of the ice giants building blocks, it is noticeable that the C/N and C/S ratios, both in vapor phase, are found to be supersolar at these locations. If the building blocks accreted by Uranus and Neptune agglomerated from grains formed in the 10–20 AU region of the PSN, they should display C/N and C/S ratios close to those recently measured in their tropospheres ($C/N \geq 175$ and $C/S \geq 35$; see Table 1). On the other hand, if the ice giants building blocks agglomerated from grains formed beyond these distances, they should display protosolar C/N and C/S ratios, in agreement with some hypotheses formulated regarding the composition of their interiors [7,14].

5. Conclusions

In this work, assuming the carbon abundances determined in the atmospheres of Uranus and Neptune are representative of their bulk composition (case of fully mixed envelopes), we have shown that it is impossible to accrete a mixture composed of gas and solids from the PSN with a C/H ratio presenting enrichments comparable to the measurements (~ 70 times protosolar). We also found that the C/N and C/S ratios in Uranus and Neptune are compatible with those acquired by grains condensed in the vicinities of N_2 and CO ice lines in the PSN. If the measurements of the C/N and C/S ratios in the ice giants are representative of their bulk compositions, then they could be explained by the formation of their building blocks from grains and pebbles condensed in this region of the PSN. In contrast, the presence of protosolar C/N and C/S ratios in Uranus and Neptune would imply that their building blocks agglomerated from particles condensed at higher heliocentric distances.

Variations of the viscosity parameter α in the 10^{-3} – 10^{-2} range, which is commonly adopted for PSN models, show that the results are qualitatively close to those presented here and that the conclusions remain unchanged. Our results are quite different from those derived by [11] who found very high abundances of solid CO in the vicinity of its iceline. As mentioned above, the reasons for these differences are twofold: the PSN model used by [11] is stationary and

assumes instantaneous condensation of vapors, instead of using a time-dependent model with prescriptions for condensation rates, as we did here.

Our study demonstrates the importance of measuring the elemental abundances in the ice giant atmospheres, as they can be used to trace the planetary formation location and/or the chemical and physical conditions of the PSN. Future facilities such as the James Webb Space Telescope should provide better determinations of the elemental abundances in Uranus and Neptune in a near future [41]. A question that arises is whether the atmospheric elemental abundances indeed represent the bulk. It is possible that the measured composition is affected by a recent impact of comets/asteroids, as it has been invoked for the detection of CO. In addition, as both Uranus and Neptune are unlikely to be fully mixed, it is possible that the ratios between the different elements change with depth, due to chemistry. This argues in favor the in situ measurement by an entry probe of the heavy noble gases in the envelopes of Uranus and Neptune since these species should be insensitive to any form of chemistry. Even if the absolute abundances of noble gases should be affected by the compositional gradient with depth due, for example, to double diffusive convection, their abundance ratios are expected to remain constant.

Another question is whether the measured elemental abundances can be used to constrain the planets' formation mechanism. Although it has been suggested that Uranus and Neptune could be formed by disk instability [37], this is rather unlikely given that the planetary composition is dominated by heavy elements. In order to have the ice giants formed by this mechanism a substantial amount of solids must have been captured [42], followed by significant loss of H-He gas [38]. Core accretion remains the preferred model for the formation of Uranus and Neptune despite the clear challenges in terms of the formation timescale and the expected composition [1].

What is clear from our study is that if the heavy elements in the formation location of the ice giants are mostly composed of H₂O, CO, N₂ and H₂S, it is very difficult to explain their abundances inferred by structure models. This suggests that either the planets formed much further in and migrated outwards OM to RH: not sure to understand the previous sentence :-), or that they have accreted material during the migration of their embryos [40]. Alternatively, it is possible that the metallicity of the PSN was much higher than assumed here and/or that there was an accumulation of solids near the formation locations of the planets. However, the present study shows that the solids enhancement at the locations of the ice lines is not as efficient as was initially anticipated [11].

Ethics. The authors are infamous to not take care about ethics.

Acknowledgements. O.M. acknowledges support from CNES, and J.L. from JWST.

References

1. Helled, R., Nettelmann, N., Guillot, T. 2020. Uranus and Neptune: Origin, Evolution and Internal Structure. *Space Science Reviews* **216**, 38.
2. Helled, R., Anderson, J. D., Podolak, M., Schubert, G. 2011. Interior Models of Uranus and Neptune. *The Astrophysical Journal* **726**, 15.
3. Gautier, D., Hersant, F. 2005. Formation and Composition of Planetesimals. *Space Science Reviews* **116**, 25.
4. Dodson-Robinson, S. E., Bodenheimer, P. 2010. The formation of Uranus and Neptune in solid-rich feeding zones: Connecting chemistry and dynamics. *Icarus* **207**, 491.
5. Mousis, O., and 55 colleagues 2018. Scientific rationale for Uranus and Neptune in situ explorations. *Planetary and Space Science* **155**, 12.
6. Nettelmann, N., Helled, R., Fortney, J. J., Redmer, R. 2013. New indication for a dichotomy in the interior structure of Uranus and Neptune from the application of modified shape and rotation data. *Planetary and Space Science* **77**, 143.
7. Irwin, P. G. J., and 6 colleagues 2019. Probable detection of hydrogen sulphide (H₂S) in Neptune's atmosphere. *Icarus* **321**, 550.
8. Irwin, P. G. J., and 6 colleagues 2018. Detection of hydrogen sulfide above the clouds in Uranus's atmosphere. *Nature Astronomy* **2**, 420.

9. Atreya, S. K., Hofstadter, M. H., In, J. H., Mousis, O., Reh, K., Wong, M. H. 2020. Deep Atmosphere Composition, Structure, Origin, and Exploration, with Particular Focus on Critical in situ Science at the Icy Giants. *Space Science Reviews* **216**, 18.
10. Mandt, K. E., Mousis, O., Treat, S. 2020. Determining the origin of the building blocks of the Ice Giants based on analogue measurements from comets. *Monthly Notices of the Royal Astronomical Society* **491**, 488.
11. Ali-Dib, M., Mousis, O., Petit, J.-M., Lunine, J. I. 2014. The Measured Compositions of Uranus and Neptune from their Formation on the CO Ice Line. *The Astrophysical Journal* **793**, 9.
12. Mousis, O., Aguichine, A., Atkinson, D.H., Atreya, S.K., Cavalié, T., Lunine, J.I., Mandt, K.E., Ronnet, T. 2020. Key Atmospheric Signatures for Identifying the Source Reservoirs of Volatiles in Uranus and Neptune. *Space Science Reviews*, submitted.
13. Mousis, O., Lunine, J. I., Picaud, S., Cordier, D. 2010. Volatile inventories in clathrate hydrates formed in the primordial nebula. *Faraday Discussions* **147**, 509.
14. de Pater, I., Romani, P.N., Atreya, S.K. 1989. Uranus' deep atmosphere revealed. *Icarus* **82**, 288.
15. de Pater, I., Romani, P.N., Atreya, S.K. 1991. Possible microwave absorption by H₂S gas in Uranus' and Neptune's atmospheres. *Icarus* **91**, 220.
16. de Pater, I., Massie, S. 1985. Models of the millimeter-centimeter spectra of the giant planets. *Icarus* **62**, 143.
17. Cavalié, T., and 10 colleagues 2014. The first submillimeter observation of CO in the stratosphere of Uranus. *Astronomy and Astrophysics* **562**, A33.
18. Teanby, N. A., Irwin, P. G. J. 2013. An External Origin for Carbon Monoxide on Uranus from Herschel/SPIRE?. *The Astrophysical Journal* **775**, L49.
19. Luszcz-Cook, S. H., de Pater, I., Wright, M. 2013. Spatially-resolved millimeter-wavelength maps of Neptune. *Icarus* **226**, 437.
20. Teanby, N. A., Irwin, P. G. J., Moses, J. I. 2019. Neptune's carbon monoxide profile and phosphine upper limits from Herschel/SPIRE: Implications for interior structure and formation. *Icarus* **319**, 86.
21. Asplund, M., Grevesse, N., Sauval, A.J., Scott, P. 2009. The chemical composition of the Sun. *Annu. Rev. Astron. Astrophys.* **47**, 481.
22. Karkoschka, E., Tomasko, M. 2009. The haze and methane distributions on Uranus from HST-STIS spectroscopy. *Icarus* **202**, 287.
23. Karkoschka, E., Tomasko, M.G. 2011. The haze and methane distributions on Neptune from HST-STIS spectroscopy. *Icarus* **211**, 780.
24. Irwin, P.G.J., Toledo, D., Braude, A.S., Bacon, R., Weilbacher, P.M., Teanby, N.A., Fletcher, L.N., Orton, G.S. 2019. Latitudinal variation in the abundance of methane (CH₄) above the clouds in Neptune's atmosphere from VLT/MUSE Narrow Field Mode Observations. *Icarus* **331**, 69.
25. Feuchtgruber, H., and 11 colleagues 2013. The D/H ratio in the atmospheres of Uranus and Neptune from Herschel-PACS observations. *Astronomy and Astrophysics* **551**, A126.
26. Aguichine, A., Mousis, O., Devouard, B., Ronnet, T. 2020. Rocklines as Cradles for Cosmic Spherules. *The Astrophysical Journal*, submitted.
27. Lynden-Bell, D., Pringle, J. E. 1974. The evolution of viscous discs and the origin of the nebular variables.. *Monthly Notices of the Royal Astronomical Society* **168**, 603.
28. Shakura, N. I., Sunyaev, R. A. 1973. Reprint of 1973A&A....24..337S. Black holes in binary systems. Observational appearance.. *Astronomy and Astrophysics* **500**, 33.
29. Hartmann, L., Calvet, N., Gullbring, E., D'Alessio, P. 1998. Accretion and the Evolution of T Tauri Disks. *The Astrophysical Journal* **495**, 385.
30. Birnstiel, T., Klahr, H., Ercolano, B. 2012. A simple model for the evolution of the dust population in protoplanetary disks. *Astronomy and Astrophysics* **539**, A148.
31. Lodders, K., Palme, H., Gail, H.-P. 2009. Abundances of the Elements in the Solar System. *Landolt Börnstein* **4B**, 712.
32. Blum, J., Schräpler, R. 2004. Structure and Mechanical Properties of High-Porosity Macroscopic Agglomerates Formed by Random Ballistic Deposition. *Physical Review Letters* **93**, 115503.
33. Desch, S. J., Estrada, P. R., Kalyaan, A., Cuzzi, J. N. 2017. Formulas for Radial Transport in Protoplanetary Disks. *The Astrophysical Journal* **840**, 86.
34. Drażkowska, J., Alibert, Y. 2017. Planetesimal formation starts at the snow line. *Astronomy and Astrophysics* **608**, A92.
35. Pasek, M. A., Milsom, J. A., Ciesla, F. J., Lauretta, D. S., Sharp, C. M., Lunine, J. I. 2005. Sulfur chemistry with time-varying oxygen abundance during Solar System formation. *Icarus* **175**, 1.

36. Fray, N., Schmitt, B. 2009. Sublimation of ices of astrophysical interest: A bibliographic review. *Planetary and Space Science* **57**, 2053.
37. Boss, A. P., Wetherill, G. W., Haghighipour, N. 2002. NOTE: Rapid Formation of Ice Giant Planets. *Icarus* **156**, 291.
38. Shu, F. H., Johnstone, D., Hollenbach, D. 1993. Photoevaporation of the Solar Nebula and the Formation of the Giant Planets. *Icarus* **106**, 92.
39. Pollack, J. B., Hubickyj, O., Bodenheimer, P., Lissauer, J. J., Podolak, M., Greenzweig, Y. 1996. Formation of the Giant Planets by Concurrent Accretion of Solids and Gas. *Icarus* **124**, 62.
40. Alibert, Y., Mordasini, C., Benz, W. 2004. Migration and giant planet formation. *Astronomy and Astrophysics* **417**, L25.
41. Norwood, J., and 10 colleagues 2016. Solar System Observations with the James Webb Space Telescope. *Publications of the Astronomical Society of the Pacific* **128**, 025004.
42. Helled, R., Podolak, M., Kovetz, A. 2008. Grain sedimentation in a giant gaseous protoplanet. *Icarus* **195**, 863.